CFD Simulation of Mixing and Segregation of Binary Solid Mixtures in a Dense Fluidized Bed

Anicic, Bozidar; Lu, Bona; Lin, Weigang; Wu, Hao; Dam-Johansen, Kim; Wang, Wei

Published in:
The Canadian Journal of Chemical Engineering

Link to article, DOI:
10.1002/cjce.23561

Publication date:
2020

Document Version
Peer reviewed version

CFD Simulation of Mixing and Segregation of Binary Solid Mixtures in a Dense Fluidized Bed

Bozidar Anicic,[1,2,3] Bona Lu,[3,4,*] Weigang Lin,[1] Hao Wu,[1,*] Kim Dam-Johansen,[1] Wei Wang[3,4]

[1]Department of Chemical and Biochemical Engineering, Technical University of Denmark, Søltofts Plads, Building 229, Kongens Lyngby, Denmark

[2]Sino-Danish Centre for Education and Research, 380 Huaibeizhuang, Huairou district, Beijing, China

[3]Sino-Danish College, University of Chinese Academy of Science, Huairou district, Beijing, China

[4]Institute of Process Engineering, Chinese Academy of Sciences, Beijing, China

*Corresponding authors' emails: bnlu@ipe.ac.cn; haw@kt.dtu.dk

ABSTRACT

The mixing and segregation behaviour of binary solid mixtures has been extensively studied through various experiments, while accurate CFD simulations are difficult to achieve due to process complexity and a lack of reliable constitutive relations. In this study, CFD simulations of a dense fluidized bed with glass and polystyrene particles were performed in order to identify a universal set of simulation parameters and models for simulating binary mixtures with different mixed and segregation behaviour. Through a comparison to experimental data, it was found that the EMMS drag model coupled with the Ma-Ahmadi solid pressure and radial distribution models predicted more a reasonable axial distribution of solid phases than the Syamlal O´Brien drag model coupled with the Lun et al. solid pressure and radial distribution models. The increase in the solid-solid drag further improved the simulation results.

KEYWORDS: binary mixture, CFD, drag coefficient, EMMS, solid-solid drag

INTRODUCTION

Fluidized beds are widely used in various industrial processes ranging from oil production, energy production, pharmaceutical production, high grade chemicals

This article has been accepted for publication and undergone full peer review but has not been through the copyediting, typesetting, pagination and proofreading process, which may lead to differences between this version and the Version of Record. Please cite this article as doi: 10.1002/cjce.23561.

production, etc.[1] Solid particles in these industrial processes commonly have dissimilar properties such as different particle sizes and/or densities. Such particle polydispersity leads to segregation phenomena in fluidized beds, especially in low-velocity dense fluidization such as bubbling fluidization, thus significantly influencing momentum transfer and reaction performance. The extent of segregation depends on the particle properties and operating parameters (gas velocity, volume ratio between particles, etc.).[2,3] A proper understanding of the segregation and mixing behaviour of polydisperse systems is crucial for industrial operation and process optimization.

The segregation and mixing behaviour of binary particles has been extensively investigated through various experiments.[1–8] It is commonly observed that heavier and larger particles (jetsam) tend to accumulate at the bottom of the bed, while the lighter and smaller particles (flotsam) accumulate in the upper part of the bed.[1,5] The extent of segregation is increased with a lower gas velocity,[2,5] a closer mass ratio of the jetsam and flotsam phases,[1,3] and a larger difference in the size and density of the solid phases (density being more important).[5]

In recent years, computational fluid dynamics (CFD) has emerged as a powerful tool to improve our understanding of segregation and mixing behaviour in polydisperse systems.[9–14] Among various CFD approaches, the Eulerian approach, which assumes fluid and solid particles as different continuous and fully interpenetrating phases, is widely used for industrial applications, due to its significantly lower computational cost. The simulation of the mixing and segregation of solid phases by the Eulerian approach is influenced significantly by the solid-solid drag model,[15] the gas-solid drag model,[10,11] and the particle-wall interaction.[12,13] It has been shown that a modification of the Syamlal O'Brien solid-solid drag model by Chao et al.[15,16] performed better than other solid-solid drag models for simulating a binary solid mixture of glass particles with different diameters.[11,15] For gas-solid drag models, the EMMS-based drag model was found to predict the mixing and segregation behaviour of a binary solid mixture with different size but same density particles better than conventional gas-solid drag models included in Ansys® Fluent software.[11,17] However, a universal gas-solid drag model that can be applied to a wide range of operating conditions is still not available.[10] For particle-wall interaction, the commonly used model is the Johnson-Jackson model, where the specularity coefficient (φ) is a parameter quantifying the degree of tangential momentum transfer of the solid phase ($\varphi = 1$ denotes perfectly diffused collisions and $\varphi = 0$ corresponds to perfectly specular collisions).[18] It was found that a smaller specularity coefficient promoted the particle movement along the walls, thus enhancing the mixing of the two solid phases in simulation.[13] The specularity coefficient is not measurable in experiments and is usually specified empirically based on wall roughness, the physical properties of particles, the collision velocity, etc.[19]

Even though CFD simulations of binary solid mixtures have been studied, a universal set of simulation parameters and constitutive relations, which can successfully reproduce

experimental data for a wide range of operating parameters, is still not available. Therefore, it is difficult to choose an optimal set of simulation parameters in cases where no experimental data is available for model validation. In this study, binary solid phases exhibiting significantly different segregation and mixing degrees in a dense fluidized bed are simulated, and the results are compared to the experimental data from Joseph et al.[1] The impact of reactor's geometry, specularity coefficient, radial distribution function and solid pressure, gas-solid drag model, and solid-solid drag model is evaluated. An optimal combination of the simulation parameters and a reasonable scheme that can capture the segregation and mixing behaviours is proposed.

MATHEMATICAL MODELS AND SIMULATION SET-UP

Experimental Data

Experimental data are taken from Joseph et al.[1] where the mixing and segregation of glass and polystyrene particles were experimentally studied in a fluidized bed. Two sets of data are taken for simulation: glass/polystyrene = 75:25 wt.% mixture (hereafter referred to as 75:25 mixture) that resembles a high degree of mixing; and glass/polystyrene = 50:50 wt.% mixture (hereafter referred to as 50:50 mixture) that resembles significant segregation. The physical properties of the solid phases are summarized in Table 1, and the relevant operating conditions are summarized in Table 2. The mixtures were initially mixed well at a high gas velocity (U_g/U_{mf} = 3), followed by a decrease in gas velocity (U_g/U_{mf} = 1.1) in order to study the mixing and segregation behaviour. The low gas velocity was maintained for 30 min and the axial mass distributions of the solid phases were determined by so-called frozen bed analysis.[1] This was done by turning off the gas flow and dividing the settled particles into 12 sections. The mass fractions of both solid phases were determined in each of the sections and presented as a function of dimensionless height (actual height divided by total bed height).[1] The authors showed that the settling had a minor impact on the axial distribution profiles.

Hydrodynamic Model

The Eulerian multi-fluid approach was used to describe the hydrodynamics of gas-solid fluidization and Ansys® Fluent 16.2 software was employed as the solver. The relevant governing equations are given below, while more detailed explanations can be found in Ansys documentation.[20]

The continuity equations for gas and solid phases (i = glass, polystyrene) without a consideration of mass transfer are, respectively, as follows:

$$\frac{\partial}{\partial t}\left(\varepsilon_g \rho_g\right) + \nabla \cdot \left(\varepsilon_g \rho_g \boldsymbol{u}_g\right) = 0 \qquad (1)$$

$$\frac{\partial}{\partial t}(\varepsilon_{si}\rho_{si}) + \nabla \cdot (\varepsilon_{si}\rho_{si}\boldsymbol{u}_{si}) = 0 \qquad (2)$$

$$\varepsilon_{\mathrm{g}} + \sum_i \varepsilon_{si} = 1 \qquad (3)$$

The momentum conservation equations for the gas and solid phases (i = glass, polystyrene; k = polystyrene, glass) are, respectively, as follows:

$$\frac{\partial}{\partial t}\left(\varepsilon_{\mathrm{g}}\rho_{\mathrm{g}}\boldsymbol{u}_{\mathrm{g}}\right) + \nabla \cdot \left(\varepsilon_{\mathrm{g}}\rho_{\mathrm{g}}\boldsymbol{u}_{\mathrm{g}}\boldsymbol{u}_{\mathrm{g}}\right) = -\varepsilon_{\mathrm{g}}\nabla p + \nabla \cdot \boldsymbol{\tau}_{\mathrm{g}} + \varepsilon_{\mathrm{g}}\rho_{\mathrm{g}}\boldsymbol{g} + \sum_i \beta_i\left(\boldsymbol{u}_{si} - \boldsymbol{u}_{\mathrm{g}}\right) \qquad (4)$$

$$\frac{\partial}{\partial t}(\varepsilon_{si}\rho_{si}\boldsymbol{u}_{si}) + \nabla \cdot (\varepsilon_{si}\rho_{si}\boldsymbol{u}_{si}\boldsymbol{u}_{si}) = -\varepsilon_{si}\nabla p - \nabla p_{si} + \nabla \cdot \boldsymbol{\tau}_{si} + \varepsilon_{si}\rho_{si}\boldsymbol{g} + \beta_i\left(\boldsymbol{u}_{\mathrm{g}} - \boldsymbol{u}_{si}\right) + \zeta_{ki}(\boldsymbol{u}_{sk} - \boldsymbol{u}_{si}) \quad (5)$$

Gas stress tensor:

$$\boldsymbol{\tau}_{\mathrm{g}} = \varepsilon_{\mathrm{g}}\mu_{\mathrm{g}}\left[\nabla \boldsymbol{u}_{\mathrm{g}} + \left(\nabla \boldsymbol{u}_{\mathrm{g}}\right)^T\right] - \frac{2}{3}\varepsilon_{\mathrm{g}}\mu_{\mathrm{g}}\nabla \cdot \boldsymbol{u}_{\mathrm{g}}\boldsymbol{I} \quad (6)$$

Solid stress tensor:

$$\boldsymbol{\tau}_{si} = \varepsilon_{si}\mu_{si}[\nabla \boldsymbol{u}_{si} + (\nabla \boldsymbol{u}_{si})^T] + \varepsilon_{si}\left(\lambda_{si} - \frac{2}{3}\mu_{si}\right)\nabla \cdot \boldsymbol{u}_{si}\boldsymbol{I} \qquad (7)$$

The kinetic theory of granular flow (KTGF) has been recognized as a reliable way of closing the solid phase stress for rapid granular flow.[21] When more than one solid phase are calculated, the solid phase stress for one solid phase is influenced by the presence of other solid phases.[16,22,23] At present, there are three main ways to simulate binary particle mixtures in the Eulerian framework: 1) the binary particles are treated as two solid phases and each solid phase uses the KTGF for monosized particles to calculate the solid phase stress, with the influence of other solid phases considered in the radial distribution function; 2) the binary particles are treated as two solid phases but the KTGF-based closures are modified to consider the polydispersity;[11,15,25] and 3) the binary particles are treated as one solid phase but the KTGF used in the simulation considers the influence of polydispersity.[27] The first approach is often used in the simulation of binary systems due to its relatively high computational stability.[17,24] For the experimental system used in our simulation, van Wachem et al.[26] and Joseph et al.[1] stated that at low velocities segregation is expected to be predominantly caused by particle drag and gravity with granular temperature and granular pressure playing a negligible role. Thus, this study attempts to employ the first approach.

An algebraic form of the granular temperature transport equation is used. The Syamlal O′Brien model can be used to determine collisional and kinetic viscosities,[29]the Schaeffer′s model to determine frictional viscosity,[30] and bulk viscosity employs the Lun et al. model.[27] For radial distribution and solid pressure, the Lun et al.[27] models

and the models developed by Ahmadi and Ma[28] are used. The Ma-Ahmadi models are particularly applicable to dense fluidized bed systems, where the particle-particle interactions are important.[28] Table 3 lists the different models for solid pressure, radial distribution function, solid-solid drag, and gas-solid drag that are investigated in this study, and details for other KTGF closures are provided in the Ansys documentation.[20]

Several gas-solid drag models are available in the Ansys® Fluent software. The Syamlal O′Brien model is a gas-solid drag model that has been recently used for the simulation of multi-phase systems.[13] In addition, the heterogeneous EMMS-bubbling model for dense fluidization is also commonly used.[32] In the EMMS-bubbling model, the heterogeneity indexes (H_D) representing the disparity between the homogeneous and heterogeneous drag coefficients are obtained by inputting operating conditions and phase parameters (gas velocity density and viscosity, mean solid density, and mean solid diameter).[32] The average physical properties for the two investigated solid phases are similar, therefore, the same set of H_D (given by Equation (15)) is used for both phases:

$$H_D = \begin{cases} 1 \ (\varepsilon_g < 0.4176) \\ -22\,980 + 211\,550\varepsilon_g - 727\,758{\varepsilon_g}^2 + 1\,118\,110{\varepsilon_g}^3 - 642\,017{\varepsilon_g}^4 \ (0.4161 < \varepsilon_g < 0.446) \\ -19.75 + 153.17\varepsilon_g - 445.39{\varepsilon_g}^2 + 567.69{\varepsilon_g}^3 - 271.94{\varepsilon_g}^4 \ (0.446 < \varepsilon_g < 0.628) \\ 1 \ (0.628 < \varepsilon_g < 0.999) \end{cases} \quad (15)$$

Simulations Settings

Figure 1 shows the 2D and 3D geometries of the fluidized bed, with the meshes generated by the Ansys® ICEM 17.2. For the 2D domain, the cell size is 2 × 4 mm, giving a total of 9000 cells in the domain. For the 3D domain, the total number of cells is 155 375. The height of the 3D domain was reduced in order to reduce the number of cells because the 2D simulation showed that there were no solid particles above 250 mm height. The cell size was set below $10d_s$ based on the recommendations provided in the literature.[12] It has been shown further decrement in cell size below $10d_s$ has no significant impact on the simulation results,[33] therefore, the grid-dependence study was not performed. The solid mixture was initially packed (as marked in Figure 1) before the fluidizing air was introduced. The air inlet velocity was set to the value given in Table 2. The non-slip boundary condition was prescribed for the gas phase. On the other hand, the partial-slip boundary condition with three different specularity coefficients (φ = 0.5, 0.05, and 0.0005) were specified for the solid phases. Transient simulations were performed and started with the time step of 0.0001 s, followed by a gradual increase to 0.001 s. The total simulation time was 200 s, with the last 50 s being used for data averaging. We used higher order discretization schemes in our simulations because they are commonly used for multi-phase systems.[12,13]

The parameters and models selected for all of the investigated simulation cases are summarized in Table 4. The impact of the geometry was first investigated because it was suggested that using 3D geometry can reproduce the behaviour of the bubbles more precisely,[34,35] and bubbles play a significant role in the mixing of solid mixtures. Furthermore, the effect of the gas-solid drag model was investigated since it was shown that the gas-solid drag model plays an important role in capturing the segregation of binary solid particles.[10] The effect of the boundary conditions was evaluated by modifying the specularity coefficient values since a lower value would enable movement along the walls and, consequently, promote the mixing.[13] The influence of the solid stress tensor was investigated by changing the solid pressure and radial distribution models since the correct modelling of solid stress tensor is important in dense systems. Finally, the influence of the solid-solid drag model was investigated by multiplying the solid-solid drag coefficient, ζ_{ki}, with an additional constant (hereafter denoted by SS) that varied between 0.25–4. Values higher than 1 indicate that the interaction between the solid phases is enhanced, which might be important in dense systems.

SIMULATION RESULTS

Base Case Simulation

Figure 2 presents a comparison between the base case simulation results and the experimental data.

For the 75:25 mixture, the axial profile of the glass mass fraction predicted by the base case simulation differs significantly from the experimental data. The simulation shows that the glass and polystyrene particles are well-mixed in the lower part of the bed, and the mass fraction of the glass is slightly decreased as the bed height increases. In the upper part of the bed, the glass mass fraction is decreased significantly and almost no glass is present at the top of the bed. In contrast, the experiments show that the partial segregation of the glass phase only occurs in the bottom of bed, while a relatively constant mixing degree is observed in the upper part of the bed (above 0.2 dimensionless height). It should be pointed out that during the transient simulation alternate mixing/segregation of two solid phases in the upper part of reactor was observed. The glass mass fraction in the upper part of the reactor followed an alternating scheme of lower and higher mass fractions, each of 4–5 s (fluctuation around the average value shown at Figure 2). Such behaviour is less probable in actual systems, which further indicates that the base case simulation settings cannot successfully reproduce the chosen experimental data. For the 50:50 mixture, the obtained mass fraction of glass in the axial direction is closer to the experimentally observed profile. The simulation captures the experimental segregation trends (the segregation of glass in the lower part of the bed, while the upper part is polystyrene rich), even though they do not provide the same quantitative data. The simulation results in Figure 2 indicate that the base case may

successfully reproduce the binary solid mixtures where significant phase segregation occurs, while its implementation for relatively well-mixed systems is limited.

Comparison of 2D and 3D Geometry

3D simulations were performed for the 75:25 mixture and the results are presented in Figure 3. It was found that the results for the 2D and 3D geometries are very similar in most regions. It is commonly suggested that the properties of bubbles can be reproduced best using 3D geometry,[34,35] however, both 2D and 3D simulations can capture main flow features such as axial profiles in fluidized beds.[33] Based on the similar results shown in Figure 3, the 2D geometry is used in further investigations due to its significantly lower computational cost.

Impact of Specularity Coefficient

Figure 4 compares the simulation results using different particle-wall boundary conditions by changing the specularity coefficient. For the 75:25 mixture, the impact of the specularity coefficient on the axial distribution is minor, even though a lower value promoted the mixing slightly.[13] For the 50:50 mixture, the impact of the specularity coefficient seems to be more pronounced with the overall mixing degree decreased and a higher specularity coefficient value (0.5). The glass mass fraction decreases monotonously with elevation for a higher value of specularity coefficient (0.5), and a nearly complete segregation of polystyrene occurs at the top of the bed. This finding is in agreement with previous studies that have shown that higher specularity coefficient values can promote phase segregation (observed only for the 50:50 mixture).[12,13] In our case, it is found that the experimental and simulation results with $\varphi = 0.05$ are comparable, and thus this value is used in further simulations.

Effects of Gas-Solid Drag Model

Figure 5 provides a comparison between the simulation results of different gas-solid drag models. It should be noted that the computational time to simulate the cases of the EMMS-bubbling drag model is ~20 % longer than the base case simulations since more iteration steps are necessary for convergence.

For the 75:25 mixture, the gas-solid drag model has a significant impact on the simulation results. When using the EMMS drag model, a significant segregation of the two solid phases is observed. The glass mass fraction in the bottom part of the bed is almost equal to 1, while the solid mixture in the upper part of the bed is rich in polystyrene and its mass fraction slightly increases in the upper part of the bed. There is still a significant difference between the simulation results of the EMMS drag model and the experimental data. However, at least the partial segregation of the heavier phase (glass) in the lower part of the bed is captured by the simulation. On the other hand, the

mixing degree of the solid phases in upper part of the bed is much lower compared to the experimental data.

For the 50:50 mixture, the overall segregation of the two phases is more pronounced with the EMMS drag model. Glass is mainly found in the lower part of the bed with only a small amount mixed with the polystyrene in the upper part. The trends of the simulation, i.e., glass-rich lower part and polystyrene-rich upper part of reactor, are similar to the experimental results, yet the experimental and simulation results are not comparable.

The performed analyses show that the gas-solid drag model has a significant impact on the simulation results in both of the investigated systems. However, the experimental and simulation data for both drag models are not quantitatively comparable. Even though the EMMS-bubbling drag model can reproduce some of the axial distribution trends better, it is still difficult to determine which gas-solid drag model is more appropriate to use. Thus, both of models are used in the further simulations.

Impact of Solid Pressure and Radial Distribution Models

Radial distribution function and solid pressure are important parameters that influence the solid stress tensor. Here, the effect of the radial distribution and solid pressure models is investigated by replacing the commonly used Lun et al.[27] models with the Ma-Ahmadi models.[28] The results obtained for both mixtures using the two gas-solid drag models are plotted in Figures 6 and 7.

For the 75:25 mixture, the Ma-Ahmadi model increased the mixing degree of the glass and polystyrene phases for both of the gas-solid drag models. Consequently, the simulation and experimental results are more comparable, especially for the EMMS gas-solid drag model. A similar influence of these models is observed for the 50:50 mixture, especially when using the EMMS gas-solid drag model. In this case, the mixing degree in the upper part of the bed is increased, which causes the simulation and experimental results to be more comparable.

The Ma-Ahmadi models consider particulate fluctuations in kinetic energy in addition to the fluid phase fluctuations, which allows accurate predictions to be made regarding solid stresses. That is why these models can be applied to the highly dense systems where particle collisions are important.[28] Since the investigated systems are dense, it is expected that the solid-solid interaction is significant or even dominant over gas-solid interactions. The implementation of the Ma-Ahmadi models to determine solid pressure and radial distribution with the EMMS gas-solid drag model significantly improves the simulation results, and therefore these models are used for further simulations.

Impact of Solid-Solid Drag Model

Solid-solid drag models are used in order to describe the momentum transfer between the solid phases during collision. The effect of solid-solid drag model is investigated by multiplying the solid-solid drag coefficient by a constant SS. The solid-solid interaction is usually underestimated in dense systems by using the Syamlal-O′Brien symmetric drag model.[31] In the early derivation of the solid-slid drag model,[31] only the collision of one particle A (first solid phase) and one particle B (second solid phase) is considered because considering multiple collisions is extremely complex. At the same time, the authors introduced a modification constant that should account for multiple collisions between particles, and the constant was later related to the radial distribution function.[31] In order to further enhance the impact of the multiple collisions at any given time, SS coefficients higher that 1 are considered when adjusting the solid-solid drag model. Results obtained after adjusting the solid-solid drag for both mixtures are given in Figure 8.

For SS equal to 4, the mixing between the solid phases is improved, which causes the simulation and experimental data to be comparable. On the other hand, a lower value of the constant (SS = 0.25) promotes segregation, as was observed for the 75:25 mixture. It seems that the impact of the coefficient is more significant for the 75:25 mixture, which is probably related to the volume ratio between the solid phases (almost 54:46 in this case). In this particular case, in which the volume of the phases is nearly equal, the solid-solid momentum exchange is significant and may determine the flow patterns.[36] The modification of the solid-solid drag models by adjusting the relevant parameters has been reported in the literature.[15] The authors arbitrarily set the value of the frictional coefficient ($C_{fr,ki}$) in the solid-solid drag model to 800 and the experimental and simulation results agreed better.[15] The collisions between the solid particles A and B at any given time are influenced by the coefficient′s values used in our case. The SS values can be related to a number of contact points between each particle A and each particle B in the dense beds. In other words, there is certain number of particles A in contact with each particle B (and vise-versa) at any time in the dense bed. The number of contact points depends on the volumetric ratio between particles A and B, as well as on their size, and they varies between 0–5.[37] This is why the further increase in the SS constant value may provide cause the simulation and experimental results to be more comparable, although it has no specific physical interpretation. The interaction between the solid phases has to be carefully considered in the future and new solid-solid drag models (in order to increase the interactions in dense multi-phase systems) have to be established. The introduction of modification coefficients is only a temporary and easy alternative.

CONCLUSION

The gas-solid drag, solid stress tensor, and solid-solid drag are important factors in the CFD simulation of binary solid mixtures in dense fluidized beds. These have to be carefully chosen in order to ensure that the experimental and simulation results are comparable for binary mixtures with different mixing and segregation patterns. Our study showed that compared to the commonly used Syamlal O'Brien gas-solid drag model coupled with the Lun et al. solid pressure and radial distribution models, the EMMS-bubbling gas-solid drag model coupled with the Ma-Ahmadi et al. solid pressure and radial distribution models can more reasonably predict the segregation and mixing behaviour of glass/polystyrene particles in dense fluidized beds. The adjustment of parameters linked to the solid-solid interaction can help to improve the simulations results. Among these factors, it is important to choose the gas-solid drag model in order to obtain accurate predictions of the dense fluidization of the binary mixture. The increase of the solid-solid friction coefficient further improves the simulation predictions. The gas-solid and solid-solid drag models considering the polydisperse features are expected to be established in the future in order to improve the simulation of the polydisperse fluidized system.

ACKNOWLDGEMENT

This project is funded by the Innovation Fund Denmark (DANCNGAS), National Natural Science Foundation of China under grant no. 21576263, 21625605, and 91834302, the "Transformational Technologies for Clean Energy and Demonstration" Strategic Priority Research Program of the Chinese Academy of Sciences (XDA21030700), the Youth Innovation Promotion Association of Chinese Academy of Sciences under grant no. 2015033, the Sino-Danish Center for Education and Research, and the Technical University of Denmark.

NOMENCLATURE

ρ	density (kg/m^3)
$\boldsymbol{u}$	velocity (m/s)
$\boldsymbol{U}$	superficial velocity (m/s)
$\boldsymbol{\tau}_{\mathrm{g}}$	stress tensor of gas phase (Pa)
$\boldsymbol{\tau}_{si}$	stress tensor of solid phase (Pa)

p	pressure (Pa)
β_i	drag coefficient between gas and solid phases (kg/(m^3·s^1))
ζ_{ki}	drag coefficient between solid phases (kg/(m^3·s^1))
θ_s	granular temperature of solid phase (m^2/s^2)
d_s	diameter of solid phase (m)
g_0	radial distribution
e_{ss}	restitution coefficient
p_s	solid pressure (Pa)
μ_g	viscosity of gas phase (Pa·s)
μ_s	viscosity of solid phase (Pa·s)
λ_s	granular bulk viscosity of solid phase (Pa·s)
λ_g	viscosity of gas phase (Pa·s)
H_D	heterogeneity index
ε_g	voidage (gas volume fraction)
ε_{si}	solid volume fraction of phase *i*
$C_{fr,ki}$	coefficient of friction between solid phases
φ	specularity coefficient

Re Reynold's number

REFERENCES

[1] G. G. Joseph, J. Leboreiro, C. M. Hrenya, A. R. Stevens, *AIChE J.* **2007**, *53*, 2804.

[2] M. J. V. Goldschmidt, J. M. Link, S. Mellema, J. A. M. Kuipers, *Powder Technol.* **2003**, *138*, 135.

[3] H. T. Jang, T. S. Park, W. S. Cha, *J. Ind. Eng. Chem.* **2010**, *16*, 390.

[4] S. Y. Wu, J. Baeyens, *Powder Technol.* **1998**, *98*, 139.

[5] P. N. Rowe, A. W. Nienow, *Powder Technol.* **1976**, *15*, 141.

[6] A. Busciglio, G. Vella, G. Micale, *Powder Technol.* **2012**, *231*, 21.

[7] M. Hemati, K. Spieker, C. Lagurei, R. Alvarez, F. A. Riera, *Can. J. Chem. Eng.* **1990**, *68*, 768.

[8] M. Wirsum, F. Fett, N. Iwanowa, G. Lukjanow, *Powder Technol.* **2001**, *120*, 63.

[9] J. Li, Z. H. Luo, X. Y. Lan, C. M. Xu, J. Sen Gao, *Powder Technol.* **2013**, *237*, 568.

[10] J. Leboreiro, G. G. Joseph, C. M. Hrenya, D. M. Snider, S. S. Banerjee, J. E. Galvin, *Powder Technol.* **2008**, *184*, 275.

[11] Q. Zhou, J. Wang, *Chem. Eng. Sci.* **2015**, *122*, 637.

[12] S. Geng, Z. Jia, J. Zhan, X. Liu, G. Xu, *Powder Technol.* **2016**, *302*, 384.

[13] H. Zhong, J. Gao, C. Xu, X. Lan, *Powder Technol.* **2012**, *230*, 232.

[14] N. Almohammed, F. Alobaid, M. Breuer, B. Epple, *Powder Technol.* **2014**, *264*, 343.

[15] Z. Chao, Y. Wang, J. P. Jakobsen, M. Fernandino, H. A. Jakobsen, *Powder Technol.* **2012**, *224*, 311.

[16] Z. Chao, Y. Wang, J. P. Jakobsen, M. Fernandino, H. A. Jakobsen, *Chem.*

Eng. Sci. **2011**, *66*, 3605.

[17] M. Lungu, Y. Zhou, J. Wang, Y. Yang, *Powder Technol.* **2015**, *280*, 154.

[18] H. Zhong, X. Lan, J. Gao, Y. Zheng, Z. Zhang, *Powder Technol.* **2015**, *286*, 740

[19] P. C. Johnson, R. Jackson, *J. Fluid Mech.* **1987**, *176*, 67.

[20] ANSYS Fluent, 17.2, ANSYS, Beijing **2016**, http://www.ansys.com/products/fluids/ansys-fluent.

[21] D. Gidaspow, *Multiphase Flow and Fluidization: Continuum and Kinetic Theory Descriptions*, Academic Press, Boston **1994**.

[22] B. Sofiane, *Chem. Eng. Sci.* **2008,** *63*, 5672.

[23] A. Nikolopoulos, N. Nikolopoulos, P. Grammelis, E. Kakaras, *Proceedings of 21st International Conference on Fluidized Bed Combustion* **2012**, *3*, 875.

[24] C. Tagliaferri, L. Mazzei, P. Lettieri, A. Marzocchella, G. Olivieri, P. Salatino, *Chem. Eng. Sci.* **2013**, *102*, 324.

[25] M. Zeneli, A. Nikolopoulos, N. Nikolopoulos, P. Grammelis, S. Karellas, E. Kakaras, *Fuel Process. Technol.* **2017**, *162*, 105

[26] B. G. M. van Wachem, J. C. Schouten, C. M. van den Bleek, R. Krishna, J. L. Sinclair, *AIChE J.* **2001**, *47*, 1292.

[27] C. K. K. Lun, S. B. Savage, D. J. Jeffrey, N. Chepurniy, *J. Fluid Mech.* **1984**, *140*, 223.

[28] G. Ahmadi, D. Ma, *Multiphase Flow* **1990**, *16*, 323.

[29] M. Syamlal, W. Rogers, T. J. O`Brien, "MFIX documentation theory guide," *NETL Multiphase Flow Science*, **2019,** accessed on 1 October 2018, https://mfix.netl.doe.gov/.

[30] D. G. Schaeffer, *J. Differ. Equations* **1987**, *66*, 19.

[31] M. Syamlal, *The Particle-Particle Drag Term in a Multiparticle Model of Fluidzation,* National Technical Information Service, Springfield 1987.

[32] K. Hong, Z. Shi, W. Wang, J. Li, *Chem. Eng. Sci.* **2013**, *99*, 191.

[33] T. Li, A. Gel, S. Pannala, M. Shahnam, M. Syamlal, *Powder Technol.*

2014, *265*, 2.

[34] N. Xie, F. Battaglia, S. Pannala, *Powder Technol.* **2008**, *182*, 1.

[35] E. Peirano, V. Delloume, B. Leckner, *Chem. Eng. Sci.* **2001**, *56*, 4787.

[36] J. Li, J. A. M. Kuipers, *Chem. Eng. Sci.* **2007**, *62*, 3249.

[37] Y.-J Hao, T. Tanaka, *Can. J. Chem. Eng.* **1988**, *66*, 761.

Figure 1 2D and 3D geometry of the simulated fluidized bed.

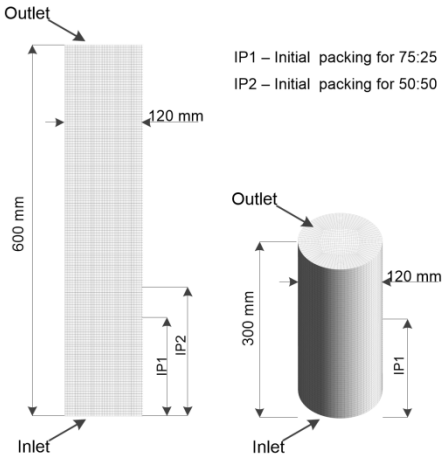

Figure 2 Comparison between simulation results and experimental data from Joseph et al.[1] for 75:25 and 50:50 mixtures.

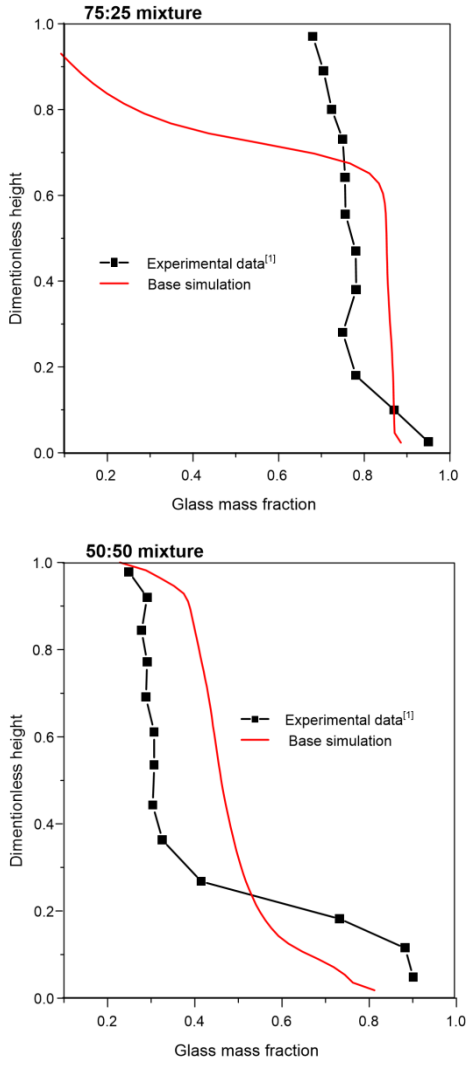

Figure 3 Comparison of 2D and 3D axial profiles together with experimental results from Joseph et al.[1] for glass/polystyrene=75/25 mixture

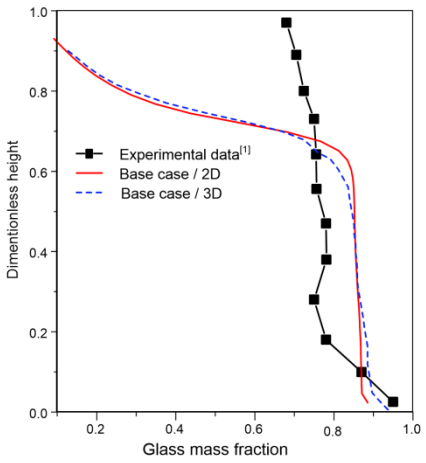

Figure 4 Impact of specularity coefficient on simulation results and comparison with experimental data from Joseph et al.[1]

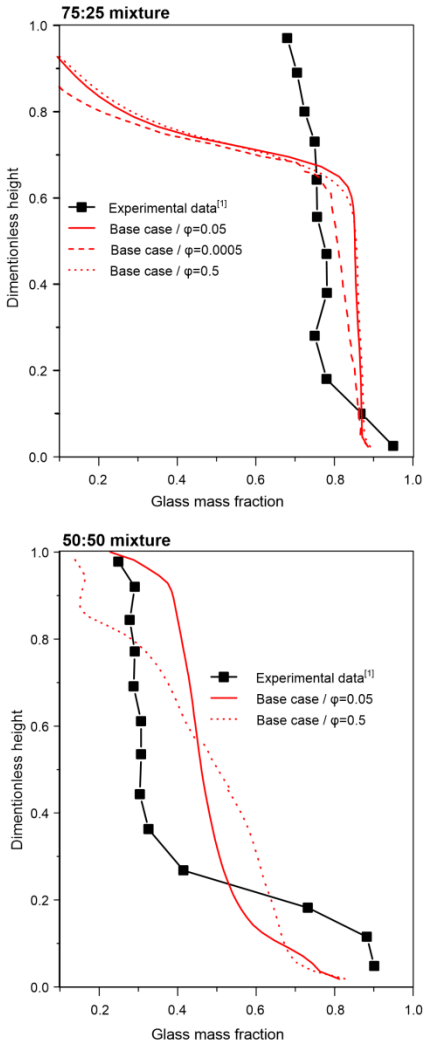

Figure 5 Comparison of axial profiles of glass mass fraction using Syamal-O'Brien and EMMS/bubbling models with experimental data from Joseph et al.[1]

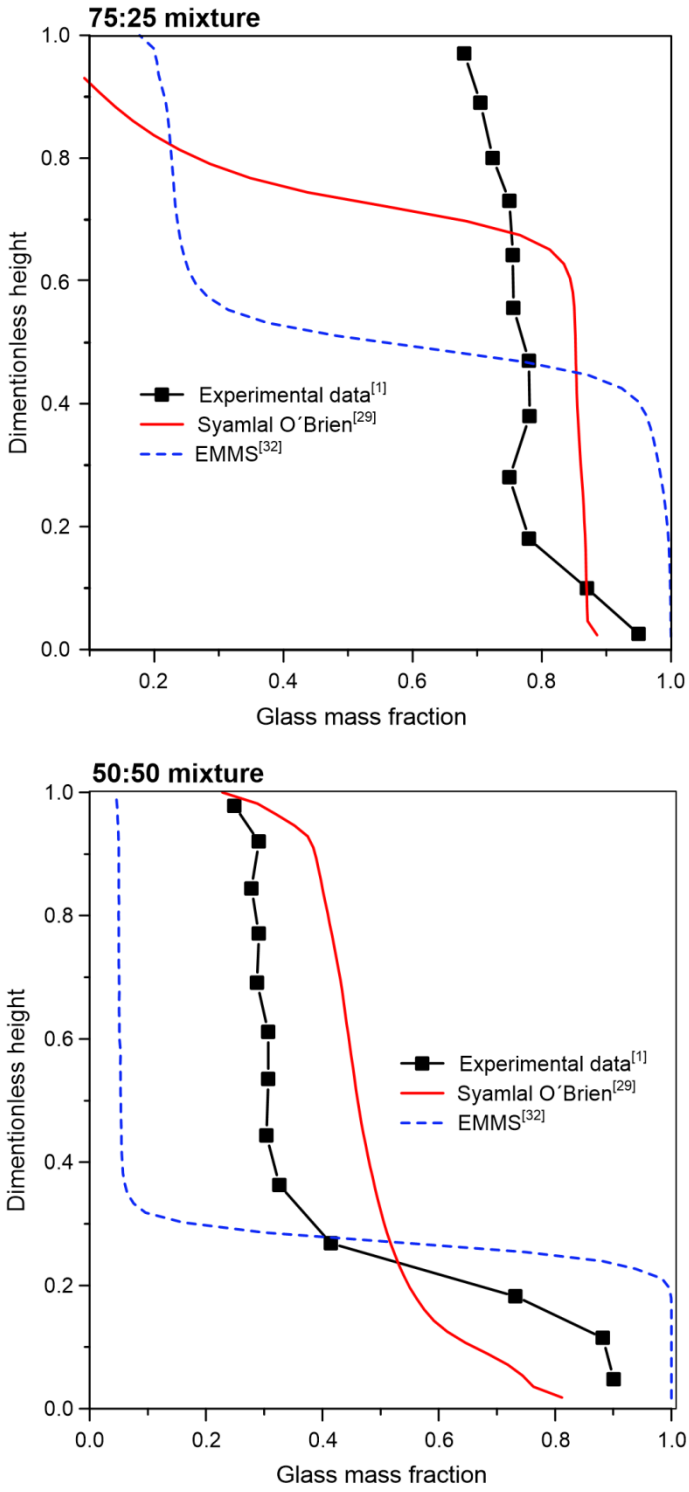

Figure 6 The impact of solid pressure and radial distribution models for 75:25 mixture and comparison with experimental data from Joseph et al.[1]

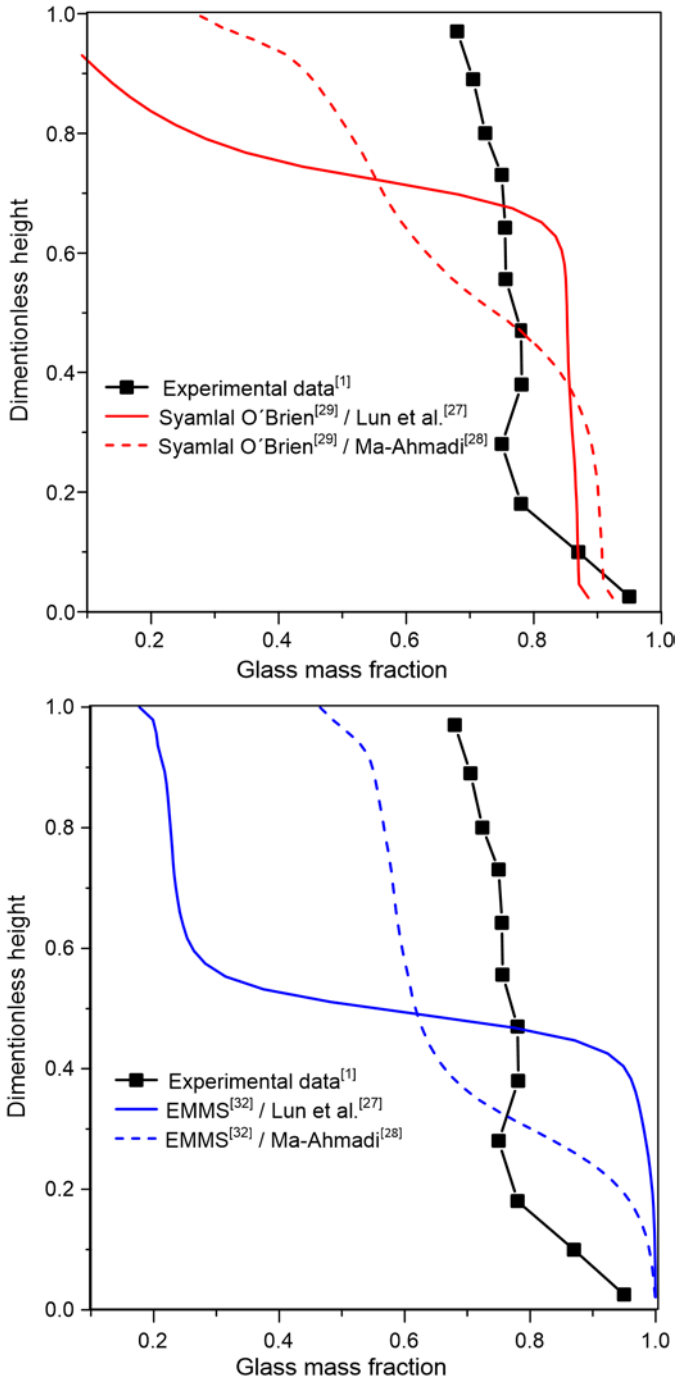

Figure 7 The impact of solid pressure and radial distribution models for 50:50 mixture and comparison with experimental data from Joseph et al.[1]

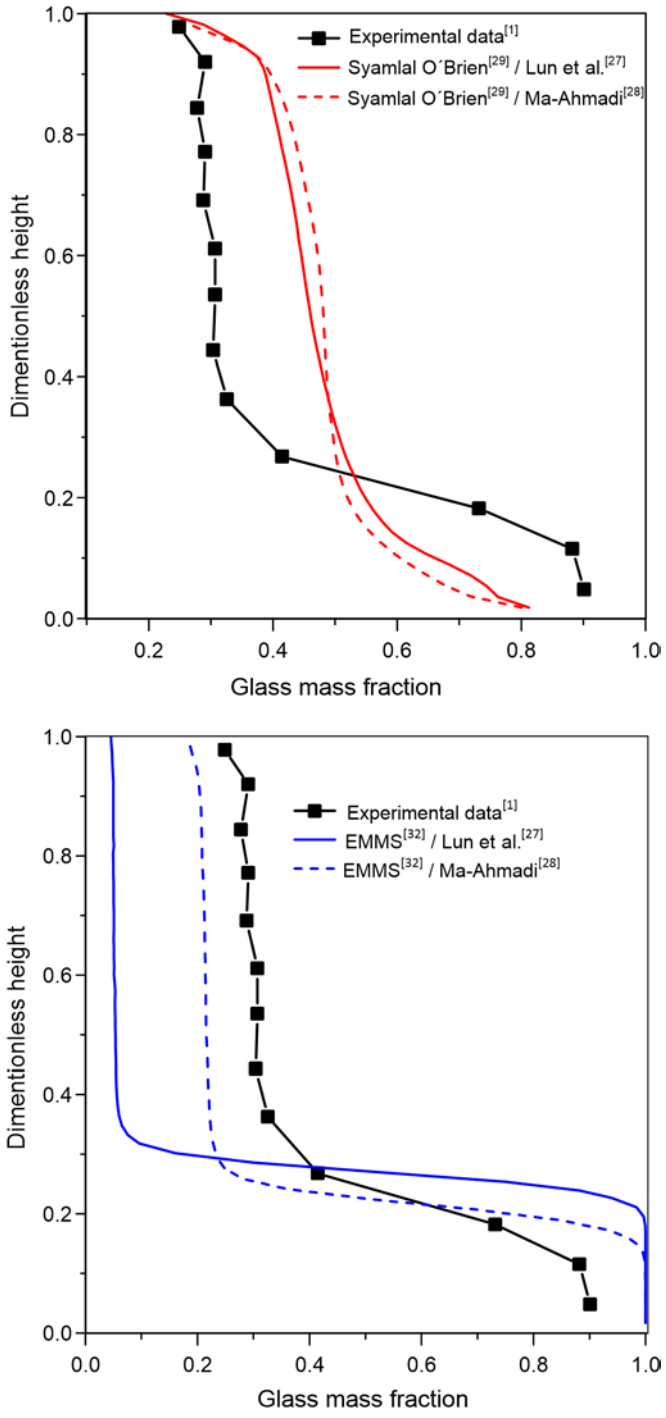

Figure 8 The impact of solid- solid drag modification and comparison with experimental data from Joseph et al.[1]

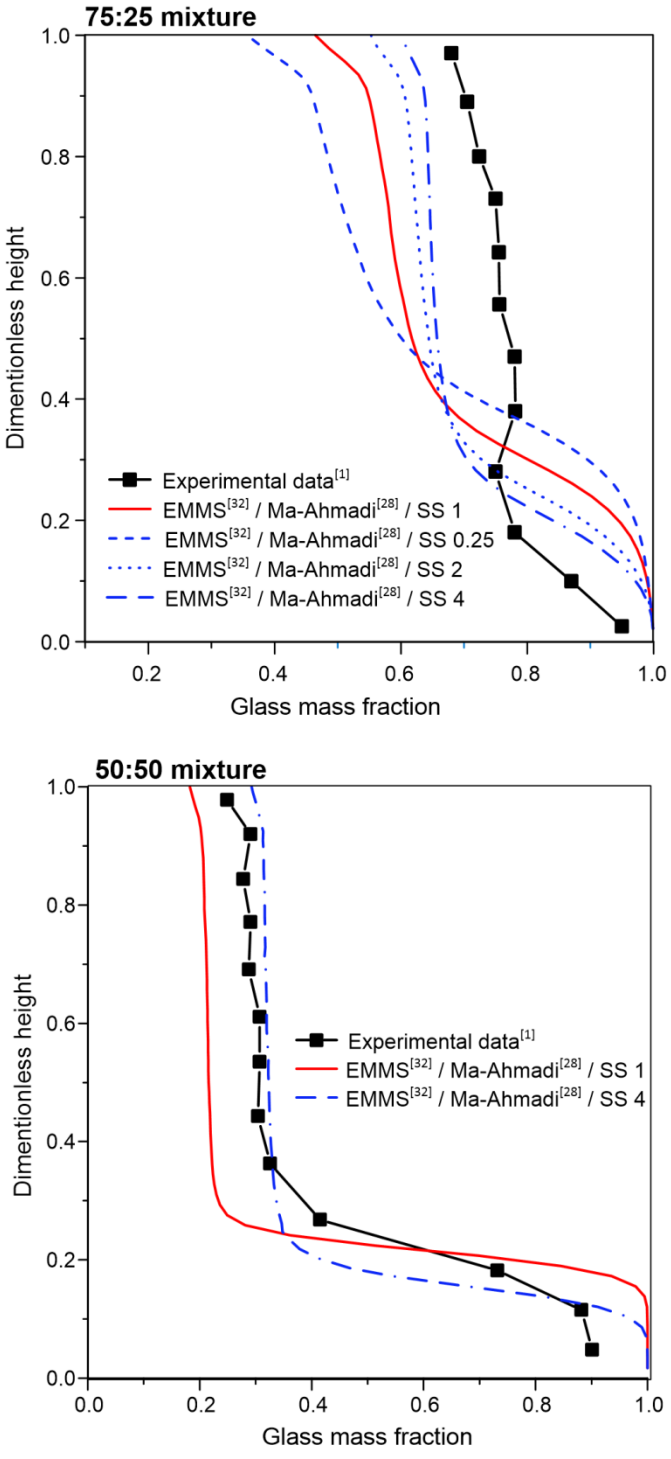

Table 1. Physical properties of the glass and polystyrene particles from Joseph et al.[1]

Material	d (μm)	ρ_s (kg/m^3)	Sphericity	U_{mf} (cm/s)
Glass	231	2476	0.944	5.6
Polystyrene	231	1064	0.981	2.9

Table 2. Main operating parameters of the experimental systems from Joseph et al.[1]

Mixture mass ratio (glass/polystyrene)	75:25	50:50
Mixture volume ratio (glass/polystyrene)	56:44	29:71
Cylinder diameter (cm)	12	12
Mass of the mixture (kg)	2	2
Minimal fluidization velocity of mixture U_{mf} (cm/s)	7.1	6.9
Superficial gas velocity U_g (cm/s)	7.81	7.59
U_g/U_{mf}	1.1	1.1
Mixture packing limit	0.585	0.572
Air density (kg/m^3)	1	1
Air viscosity (Pa·s)	$1.83 \cdot 10^{-5}$	$1.83 \cdot 10^{-5}$

Table 3. Expressions for solid pressure, radial distribution function, solid-solid drag, and gas-solid drag

Solid pressure:

Lun et al.[27]

$$p_\mathrm{s} = \varepsilon_\mathrm{s}\rho_\mathrm{s}\theta_\mathrm{s} + 2\rho_\mathrm{s}(1+e_\mathrm{ss})\varepsilon_\mathrm{s}^2 g_0\theta_\mathrm{s} \quad (8)$$

Ahmadi and Ma[28]

$$p_\mathrm{s} = \varepsilon_\mathrm{s}\rho_\mathrm{s}\theta_\mathrm{s}\left[(1+4\varepsilon_\mathrm{s}g_0) + \frac{1}{2}\left[(1+e_\mathrm{ss})\left(1-e_\mathrm{ss}+2\mu_\mathrm{s,fr}\right)\right]\right] \quad (9)$$

Radial distribution function:

Lun et al.[27]

$$g_0 = \left[1-\left(\frac{\varepsilon_\mathrm{s}}{\varepsilon_\mathrm{s,max}}\right)^{1/3}\right]^{-1} + \frac{1}{2}d_{si}\sum_{k=1}^{N}\frac{\varepsilon_{sk}}{d_{sk}} \quad (10)$$ Ma-Ahmadi [28]

$$g_0 = \frac{1+2.5\varepsilon_\mathrm{s}+4.59{\varepsilon_\mathrm{s}}^2+4.53{\varepsilon_\mathrm{s}}^3}{\left[1-\left(\frac{\varepsilon_\mathrm{s}}{\varepsilon_\mathrm{s,max}}\right)^3\right]^{0.678}} + \frac{1}{2}d_{si}\sum_{k=1}^{N}\frac{\varepsilon_{sk}}{d_{sk}} \quad (11)$$

Solid-solid drag coefficient using the Syamlal-O´Brien symmetric model[31]

$$\zeta_{ik} = \frac{3(1+e_{ik})\left(\frac{\pi}{2}+C_\mathrm{fr,ki}\frac{\pi^2}{8}\right)\varepsilon_{si}\varepsilon_{sk}\rho_{si}\rho_{sk}(d_{si}+d_{sk})^2+g_{0,ik}}{2\pi\left({\rho_{si}d_{si}}^3+{\rho_{sk}d_{sk}}^3\right)}\left|\boldsymbol{u}_{si}-\boldsymbol{u}_{sk}\right| \quad (12)$$

Gas-solid drag coefficient:

Syamlal O´Brien model[29]

$$\beta_i = \frac{3\varepsilon_\mathrm{g}\varepsilon_{si}\rho_\mathrm{g}}{4{u_\mathrm{r,}si}^2 d_{si}}C_\mathrm{D}\left(\frac{Re_{si}}{u_\mathrm{r,}si}\right)\left|\boldsymbol{u}_{si}-\boldsymbol{u}_\mathrm{g}\right| \quad (13)$$

where $u_\mathrm{r,s} = 0.5\left(A - 0.06Re_{si} + \sqrt{(0.06Re_{si})^2 + 0.12Re_{si}(2B-A)+A^2}\right)$.

For $\varepsilon_{si} \leq 0.85$, $\mathrm{A} = \varepsilon_{si}^{4.14}$, $\mathrm{B} = 0.8\varepsilon_{si}^{1.28}$; for $\varepsilon_{si} > 0.85$, $\mathrm{A} = \varepsilon_{si}^{4.14}$, $\mathrm{B} = \varepsilon_{si}^{2.65}$.

EMMS drag model[32]

$$\beta_i = \frac{3}{4} C_{\mathrm{D}0i} \frac{\varepsilon_{\mathrm{g}} \varepsilon_{\mathrm{s}} \rho_{\mathrm{g}} \varepsilon_{\mathrm{g}}^{-2.65}}{d_{si}} \left| \boldsymbol{u}_{\mathrm{g}} - \boldsymbol{u}_{\mathrm{s}i} \right| H_{\mathrm{D}} \quad (14)$$

$$\text{where} \begin{cases} C_{\mathrm{d}0i} = \frac{24\left(1+0.15 Re_{si}^{0.687}\right)}{Re_{si}}, Re_{si} < 1000 \\ C_{\mathrm{d}0i} = 0.44,\ Re_{si} \geq 1000 \end{cases}$$

Table 4. Summary of parameters investigated in this work

	Base case	Other investigated cases
Geometry	2D	3D
Gas-solid drag	Syamlal-O′Brien	EMMS-bubbling
Specularity coefficient	φ = 0.05	φ = 0.0005, 0.5
Solid pressure	Lun et al.	Ma-Ahmadi
Radial distribution function	Lun et al.	Ma-Ahmadi
Solid-solid drag	Syamlal-O′Brien symmetric (SS = 1)	Syamlal-O′Brien symmetric (SS = 0.25, 2, 4)